JEE Journal of Ecological Engineering

*Journal of Ecological Engineering*, 2025, 26(3), 48–62
https://doi.org/10.12911/22998993/199455
ISSN 2299–8993, License CC-BY 4.0

Received: 2024.11.26
Accepted: 2025.01.13
Published: 2025.02.01

# Optimized co-solvent methanolysis of mixed non-edible oils over nano solid base catalyst derived from egg shells

Baraa A. Kareem[1], Abdelrahman B. Fadhil[1*]

[1] Department of Chemistry, College of Science, Mosul University, Majmoaa Street, 41002, Mosul, Iraq
* Corresponding author's e-mail: abdelrahmanbasil@yahoo.com

## ABSTRACT

A nano solid base catalyst (NSBC) was developed from chicken egg shells (CES) and utilized in the cosolvent methanolysis (CSM) and non-solvent methanolysis (NSM) of an equal mix of non-edible oils (waste cooking oil and wild mustard oil) into biodiesel (BD) via the optimized methodology. The NSBC was synthesized by calcinating the raw CES at 850 °C for 2 h and a heating rate of 10 °C/min. The NSBC was identified using FESEM, EDX, BET surface area and pore volume, and XRD. The XRD measurement confirmed the transformation of the pristine CES into nano CaO. Also, the NSBC had a BET surface area of 11.47 $m^2/g$, while its average pore diameter was 8.12 nm, demonstrating its mesoporous structure, which is helpful for the methanolysis of lipids into BD. The CSM of mixed oils produced the highest output of BD (91.12%) using 5.0 wt.% of NSBC, 9:1 methanol: oil molar ratio, 40 wt.% of co-solvent at 60 °C for 1.5 h, while the NSM of the mixed oil produced the highest yield of BD (84.55%) at 65 °C for 2h using 5.0 wt.% of the NSBC and 12:1 methanol: oil molar ratio. Analysis of the resulting BD employing FTIR spectroscopy and TLC technique confirmed the transformation of the oils mix into BD. Moreover, $^1H$ NMR spectroscopy measurements exhibited that the conversion of mixed oils into BD amounted to 96.96%. Additionally, the fuel properties of the resulting BD samples conformed to those established for ASTM D6751 standards. In conclusion, the NSBC catalyst derived from the CES could be utilized as an effective catalyst for the methanolysis reaction of lipids. Also, incorporating the co-solvent within the reaction medium effectively reduced the experimental conditions required to achieve the highest transformation of the oils blend into BD compared to the NSM process.

**Keywords:** egg shells, nano solid base catalyst, mixed non-edible oils, co-solvent methanolysis, biodiesel: analysis of biodiesel.

## INTRODUCTION

The global energy system has relied on fossil fuels for a long time. However, the rapid use of these fuel sources has rapidly reduced stocks. Additionally, environmental contamination concerns have spurred many mitigation attempts. Accordingly, generating and applying biofuels from renewable materials could solve these issues (Mares et al., 2021). In this situation, BD is a partial or complete alternative to petroleum diesel. It can be originated from renewable sources, like vegetable oils or animal fats, consisting of alkyl esters of fatty acids. Esterification of fatty acids or transesterification (TE) of acylglycerols with primary alcohols are the main production routes of BD (Conceiçao et al., 2015). The TE, facilitated by an enzymatic, acidic, or catalyst, is the chief process for producing this fuel (Gupta and Rathod, 2018). Homogenous catalysts, including KOH, NaOH, $CH_3ONa$, $CH_3OK$, etc., are the main catalysts implemented for creating BD from various sources of lipids. However, these catalysts generate a lot of effluent during purification, making catalyst recycling problematic (Navas et al., 2020). Solid heterogeneous catalysts alleviate issues relating to the homogenous catalysts because of their renewability, reusability, and ease of separation from the reaction media. Among the heterogeneous catalysts for BD production is CaO. This solid base catalyst (SBC) possesses many merits that qualify it to be used as an alternative to other homogenous catalysts, like its superior basicity and ease of handling, besides its eco-friendly features and economic benefits (Jamil et al., 2021; Yan et al., 2009).

Various solid wastes, including mussel shells, chicken egg shells (CES), scallop shells, oyster shells, chicken bones, seashells, duck shells, and snail shells, have been implemented as cheap and natural sources for creating CaO (Ashine et al., 2023). The CES are mainly composed of 94.0 wt.% calcium carbonate ($CaCO_3$) in addition to 1.0 wt.% magnesium carbonate ($MgCO_3$) and 1.0 wt.% calcium phosphate ($Ca_3(PO_4)_2$). The rest of CES are organic components (mostly protein) and water (Sajadi et al., 2018; Tanpure et al., 2022). Consequently, the CES could be a sustainable source of $CaCO_3$, which can directly be employed or thermally treated to produce CaO. Both $CaCO_3$ and CaO can serve as catalysts or supports for active materials (Deharbe et al., 2023). On this account, CES could be utilized as a sustainable source for CaO production and considered an SBC for BD production. In comparison to other sources of CaO, like snail shells, crab shells, mussel shells, etc., the massive consumption of CES worldwide in various kinds of establishments, including bakeries, homes, and egg farms, will result in producing enormous quantities of CES, which are solid waste (Paruthi et al., 2023). So, discarding such solid waste in different open-field garbage dumps will contaminate air and water sources and disperse contagious diseases (Paruthi et al., 2023). Consequently, the waste CES could be a sustainable natural source for producing CaO, which can be implemented in various applications, including BD production. Synthesis of BD using CaO generated from the abovementioned precursors has been announced in the literature, e.g., the CES-derived CaO was tried as a SBC for producing BD from *Argemone mexicana* oil (Ashine et al., 2023). The CaO originated from the Mussel shell and was tested as an SBC for the methanolysis of castor oil to BD (Khan et al., 2022). Kedir et al., 2023 implemented snail shell-derived CaO as SBC for the TE of WCO into BD. Production of BD from edible vegetable oils is expensive and causes food shortages, making it the biggest issue in the BD market. Also, alternate triglyceride sources must be found due to the sensitive nature of creating BD from non-edible raw materials. Therefore, non-edible sources of lipids, like non-edible vegetable oils, animal lipids, and WCO, have been adopted as potential precursors for producing BD fuel (Navas et al., 2020). The manufacture of BD from WCO will aid in recycling this source of feedstocks and generating clean, renewable energy fuel, thus potentially lowering reliance on petrol-based feedstocks (Danane et al., 2022). Utilization of WCO for biofuel production can address food safety and energy crises, as well as environmental concerns due to their renewable, non-toxic, and clean combustion features. It was stated that the global production of WCO is estimated to be 16.54 million tons per year, with a production average of 4–8 million tons in China and nearly 1 million in the European Union (EU) (Mannu et al., 2019). Disposal of WCO into the environment will be associated with several negative impacts on the ecosystem. Uncontrolled discharge of WCO from various sources, including restaurants, domestic kitchen sinks, and food processing units, can cause FOG (fat, oil, and grease) formations as an outcome of interacting with wastewater elements (Usman et al., 2020). These deposits can pollute the environment besides causing pipe clogs and exposing live beings to viruses. So, dealing with such a pollutant is an energetic target. Production of BD from WCO could be a potential solution to eliminate organic waste and its negative environmental impact (Usman et al., 2020).

Among the negative concerns that accompany BD synthesis utilizing SBC is the catalyst's immiscibility between triglycerides and alcohol, which raises the production cost since it needs greater energy and time for heating and stirring, as well as necessitating a larger alcohol-to-oil ratio. Several approaches have been proposed to overcome this drawback, including adding cosolvent. Adding the cosolvent in the reaction medium decreases mass transfer limits, improves oil solubility in alcohol, and increases BD output. On the other hand, employing cosolvent improves response time while also mitigating shipping and storage concerns (Mohadesi et al., 2020). It is recommended to use a cosolvent with a boiling point close to that of the implemented alcohol in order to ensure its recycling with alcohol by the end of the reaction. Also, incorporating cosolvent within the TE reaction medium can lessen the conditions required to achieve maximum conversion of triglycerides into BD, including the amount of the catalyst and methanol: oil molar ratio, besides the TE temperature and duration (Saeed et al., 2021). According to the literature, various cosolvents were employed, like n-hexane (Nguyen et al., 2018), tetrahydrofuran (THF) (Chumuang et al., 2017), acetone (Laskar et al., 2020), di-isopropyl (Sahani et al., 2018), butanol (Navas et al., 2020), etc. Chumuang and

Punsuvon (2017) explored the methanolysis of waste cooking oil (WCO) into BD using calcium methoxide as an SBC in the presence of THF as a cosolvent. The TE of soybean oil to BD at room temperature using the snail shell-derived CaO as an SBC and acetone as a cosolvent was declared by Laskar et al. (2020). The Sr-Ln mixed oxides were employed for the methanolysis reaction of non-edible oils to BD in di-isopropyl as a cosolvent (Sahani et al., 2018). Finally, rapeseed oil was transformed into BD fuel for the methanolysis reaction using mixed oxides of Mg and Fe as an SBC and butanol as a cosolvent (Navas et al., 2020). Although the CSTE of various lipids has been announced in the literature using homogenous or heterogenous catalysts, the implementation of n-hexane as a cosolvent during the TE reaction of a mixture of non-edible lipids using an SBC, like CaO nanocatalyst, has not been yet declared, to the best of our knowledge. These issues motivated us to accomplish this research work and fill this gap.

Here, NSBC was developed from a naturally occurring source, the CES, after being calcined at 850 °C for 2 h. Various techniques were employed to identify the as-prepared NSBC. The latter was then tried in the CSM and NSM of mixed WCO+WMO to synthesize BD fuel via the optimized route. The resulting samples of BD were identified by $^1$H NMR and FTIR spectroscopy and TLC techniques. Determining the fuel properties of BD was also accomplished using the ASTM methodologies.

## MATERIALS AND METHODOLOGIES

### Materials

The WCO and waste CES were brought from the fast-food restaurants and sweet houses in Mosul City, Iraq. The wild mustard seeds were collected from the lands distributed within Mosul, north of Iraq, during the summer of 2024. All analytical reagent grade (AR) chemicals, including n-hexane, methanol, diethyl ether, acetic acid, and sodium sulfate, were purchased from Scharlau Chemicals, Spain. The wild mustard seeds were dried for 2 days under sunlight and then ground. Oil extraction from the ground seeds powder was accomplished in a Soxhlet extractor using n-hexane as a solvent for 10 h. The WCO and WMO were mixed with freshly activated sodium sulfate. After mixing, the resulting mixtures were left to settle for a day to detach any moisture in the oils, followed by filtration to separate the purified oil from the drying agent. Finally, the purified oils were preserved in a dark container for subsequent use.

### Synthesis of NSBC from CES

The collected discarded CES were washed thoroughly with tap water to eradicate dirt or organic materials, washed with distilled water (DW), and dried at 110 °C overnight. The dehydrated CES were ground and sieved with a 100-mesh sieve. Synthesis of the NSBC from the CES powder was carried out via calcinating 5.0 g of the powdered CES at various temperatures (800−950 °C) for multiple durations (1−3 h) in a muffle furnace (Isolab, Germany) at a 10 °C/min rate of heating. The produced catalysts were preserved in an airtight container for further application.

### Identification of the ideal NSBC

The X-ray diffractometer (XRD, PANalytical Empyrean) with a 2θ range of 10–80° and a scanning rate of 2°/min was implemented to examine the crystalline structure of the resulting NSBC. The surface area and pore size distribution of the NSBC were determined based on the $N_2$ adsorption-desorption isotherms at -196 °C (BELSORP MINI II, Japan). The surface morphology and elemental composition of the produced NSBC were recorded on a field emission scanning electron microscope (FESEM) combined with an energy dispersive X-ray (EDX) was implemented for this purpose at a 15 KV accelerating voltage (Tescan Mira 3 LMU FESEM-EDX, France, 2018).

### Methanolysis of mixed WCO+WMO by the NSBC

The CSM and NSM were applied to synthesize BD fuel from the oils mix using the as-created NSBC. The methanolysis reaction was accomplished in a 250 mL three-necked round-bottom flask attached to a reflux condenser, magnetic stirrer, and thermometer. A constant temperature water bath was implemented to regulate the methanolysis temperature. Firstly, the proper amount of the NSBC was mixed with methanol inside the round, and the resulting mixture was stirred at 40 °C for 30 min at a 700-rpm stirring rate. Subsequently, an equal quantities of oils was blended, and a predetermined amount of cosolvent (n-hexane) was poured into the reaction mixture The resulting mixture was stirred for a given duration at the determined temperature. Upon completion of the process, the NSBC was stripped from the reaction products by centrifugation. The resultant products were distilled to recover excess methanol and cosolvent after that, permitted to settle in a separating funnel to separate BD (upper phase) from the glycerin phase (lower phase) (Fadhil et al., 2020). The yield of BD was calculated as per Equation 1 (Altikriti et al., 2015):

$$\text{Yield of BD (\%)} = \frac{\text{Mass of BD produced}}{\text{Mass of oils blend used}} \times 100 \quad (1)$$

Exploring the influence of the working conditions, like the NSBC amount (1.0–6.0% w/w), methanol: oil molar ratio (3:1–18:1), cosolvent: methanol molar ratio (10–50 wt.% of oil), methanolysis temperature (30 °C, 40 °C, 50 °C, 60 °C, 65 °C, and 70 °C), and methanolysis period (30–180 min) on the BD output was carried out so as to optimize the experimental conditions that will produce the highest yield of BD.

### Analysis of BD from mixed oils

After the CSM and NSM of mixed WCO+WMO using the resulting NSBC, various techniques were employed to identify the pristine mix of oils and the typical BD sample. For this purpose, FTIR spectroscopy (JASCO V-630 FTIR spectrometer, USA) spectroscopy and $^{1}$HNMR spectroscopy (Bruker Biospin GmbH 400 MHz spectrometer) were implemented to verify the triglyceride conversion into its corresponding product. Also, as a rapid and easy technique to monitor the methanolysis reaction of the oils mixed into BD using the as-synthesized NSBC, thin layer chromatography (TLC) was exploited for this purpose utilizing silica gel plates and iodine vapor to visualize spots following fractionation (Fadhil et al., 2019). The $^{1}$H NMR was also implemented to quantify the conversion of the said blend of oils into BD following Eq.(2) :

$$\text{FAME (\%)} = \frac{2\text{AMe}}{3\text{ACH2}} \times 100 \quad (2)$$

where: $2A_{CH3}$ refers to the methyl ester protons integration value, while $A_{CH2}$ signifies the methylene protons integration values. Determining the fuel characteristics of the authentic oils blend, and its developed BD samples was accomplished following ASTM standard procedures. These properties included density (D @ 15.6 °C), kinematic viscosity (KV @ 40 °C), flash point (FP), pour point (PP) and acid value (AV).

## RESULTS AND DISCUSSION

### Selection of the typical catalyst

The conversion of waste CES into NSBC was accomplished via the optimized protocol. To do so, the pristine CES was calcined at various temperatures for different durations to find the best NSBC. The selection of the best NSBC depended on testing each prepared catalyst in the CSM and NSM of the oils blend at the conditions offered in the legend of each figure.

According to the outcomes in Fig. 1a, increasing the calcination temperature from 800 °C to 850 °C for 120 min enhanced the BD output for both processes. The best calcination temperature was 850 °C, suggesting that this temperature was enough for the entire transformation of CES into nano CaO. Temperatures above 850 °C diminished

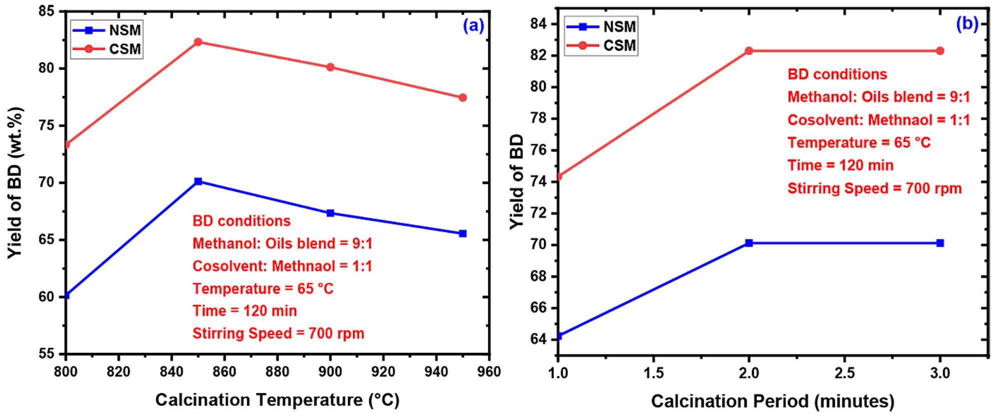

**Figure 1.** Effect of the calcination temperature and time on BD yield via CSM and NSM

the BD yield, which may be due to the sintering of the NSBC particles, leading to a reduction in the number of active sites ready for the methanolysis reaction, and thus, the BD output was reduced. Therefore, a calcination temperature of 850 °C was considered the best. Following the results presented in Figure 1b, extending the calcination time from 1 h to 2 h was associated with an increase in the BD yield via both processes, demonstrating that this period was much enough for the entire conversion of CES into CaO, while durations beyond 2 h consider a loss of energy. Therefore, a calcination period of 2h was considered the typical.

## Identification of the typical catalyst

According to the results obtained earlier, the best SBC produced from the CES was that calcined at 850 °C for 2 h. Thus, it was further identified to assess its texture, morphology, and crystalline structure.

It is well-known that the surface area and porosity of a heterogeneous catalyst potentially affect its overall performance (Huang et al., 2021). Thus, the BET surface area ($SA_{BET}$) and average pore size distribution of the resulting NSBC were determined based on the $N_2$ adsorption-desorption isotherms, which are presented in Figure 2. The $N_2$ adsorption-desorption isotherms of the resulting NSBC belonging to both samples type IV as per the IUPAC classifications, confirming the occurrence of mesoporous. This isotherm is characterized by a hysteresis loop shape, identified as type H3, with slit-shaped pores (Maneechakr and Karnjanakom, 2021). The $SA_{BET}$ of the produced NSBC amounted to 11.47 $m^2/g$, while the $SA_{BET}$ of the ES amounted to 2.35 $m^2/g$ (Annane et al., 2023). The higher $SA_{BET}$ of the resulting NSBC compared to the pristine CES could be ascribed to the hydration-dehydration reactions that occurred upon the calcination of the authentic CES at high temperatures. Moreover, the $SA_{BET}$ of the NSBC synthesized here was above that established for the CaO originated from the calcination of hollow $CaCO_3$ at 700 °C (Huang et al., 2021), which was 6.10 $m^2/g$. Nevertheless, the $SA_{BET}$ of the NSBC was below that reported for the CaO nanocatalyst synthesized via calcination of the CES at 900 °C for 3 h, which amounted to 16.40 $m^2/g$ (Pandit and Fulekar, 2017). The mean pore diameter of the as-synthesized NSBC was 8.12 nm, suggesting its mesoporous structure. It was reported that the CES-derived nano CaO had an average pore diameter of 5.07 nm (Pandit and Fulekar, 2017). According to the literature, a mesopores structure for any SBC will be suitable to provide high catalytic activity and more adsorption sites for the diffusion of the triglyceride (TG) and glycerin molecules (~2.5 nm) during the transesterification reaction (Huang et al., 2021; Zhang et al., 2017; Shan et al., 2015).

The crystalline structure of the resultant NSBC was examined through the XRD, whose pattern is offered in Figure 3. The outcomes presented in this figure suggested that the crystal structures of nano-CaO particles are analogous with major diffraction peaks for CaO at $2\theta = 32.30°$, 37.35 °, 53.90°, 64.25°, and 67.40°, which respectively belong to the crystal planes (111), (200), (220), (311), and (222). These crystal planes confirmed the entire transformation of the pristine CES into their corresponding CaO (Huang et al., 2021). Also, the observed phases were detected in the CaO nanocatalyst originating from the calcination of CES (Huang et al., 2021).

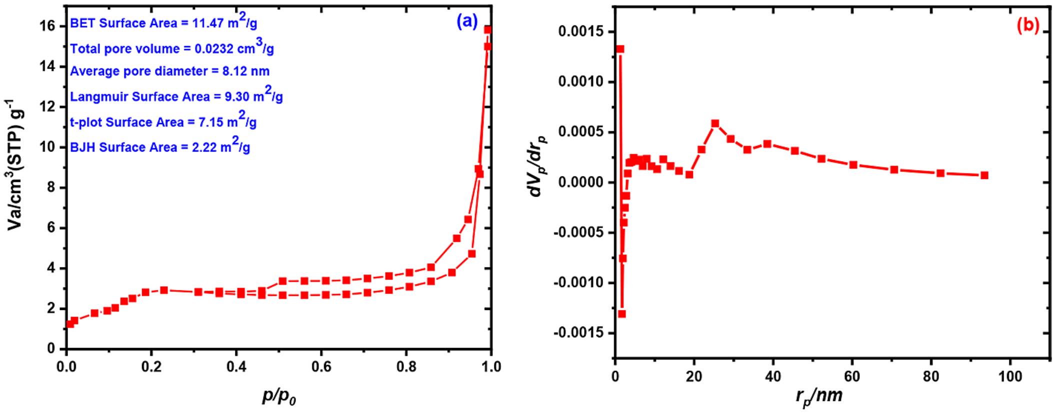

**Figure 2.** The $N_2$ adsorption-desorption isotherms, (b) pore size distribution of the CES-derived CaO catalyst

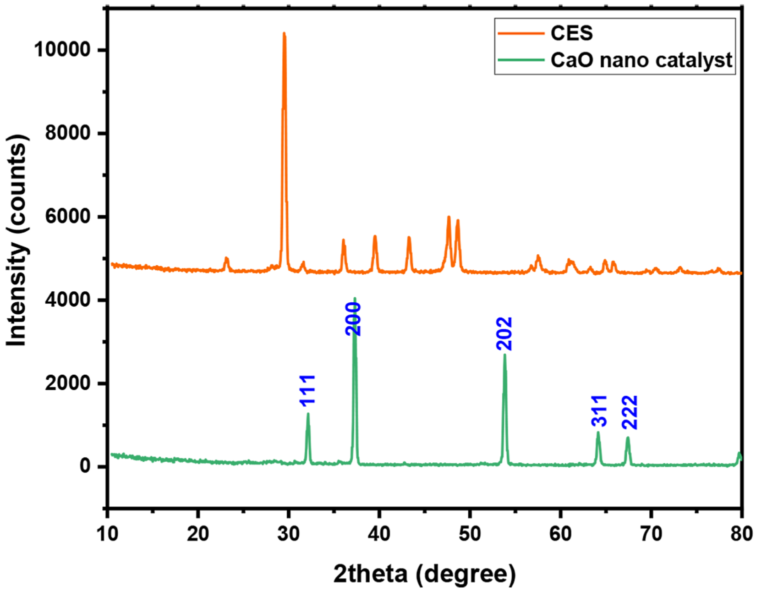

**Figure 3.** The XRD patterns of the CES-derived CaO catalyst

The crystalline size diameter (D) of CES-derived NSBC was calculated based on the Debye-Scherrer equation and was found in the range of 29.40 nm to 37.77 nm. In contrast, the average size of the CaO nanocatalyst crystalline structure, calculated following the Scherer equation, amounted to 31.16 nm. The CaO nanocatalyst derived from the calcination of CES at 900 °C exhibited an average crystalline size of 23.65 nm (Ahmad et al., 2020). Such findings confirmed the nanostructure of the as-synthesized CaO catalyst.

The surface morphology of the CES-derived CaO nanocatalyst was examined by employing FESEM. According to Figure 4, which depicts the FESEM images of the CES-derived NSBC, it showed a rough and porous surface, as it contained pores with asymmetrical sizes of semi-spherical particles, which originated as a consequence of the evolution of water and $CO_2$ gas upon thermal decomposition of $CaCO_3$ in the authentic CES at 850°C (Buasri et al., 2015). These findings were compatible with the BET measurement, confirming the porosity of the resultant CaO. Also, the particle size of the as-prepared NSBC amounted to 22.80 nm based on FESEM, which conformed with the finding deduced from the XRD measurements.

It is clear from Figure 5, which offers the EDX mapping of the CES-derived NSBC originating from the calcination of pristine CES that it was composed only of Ca and O. These outcomes confirmed that the pristine CES was totally transformed into CaO. This finding is also well-suited to the XRD analysis of the CaO catalyst, which assured the presence of CaO phases in its XRD pattern, which is in charge of the catalytic activity in the methanolysis reaction.

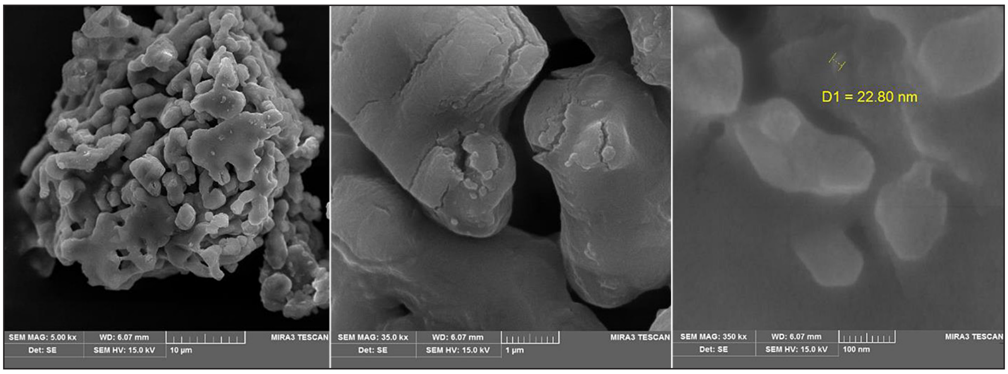

**Figure 4.** FESEM images of the CES-derived CaO catalyst

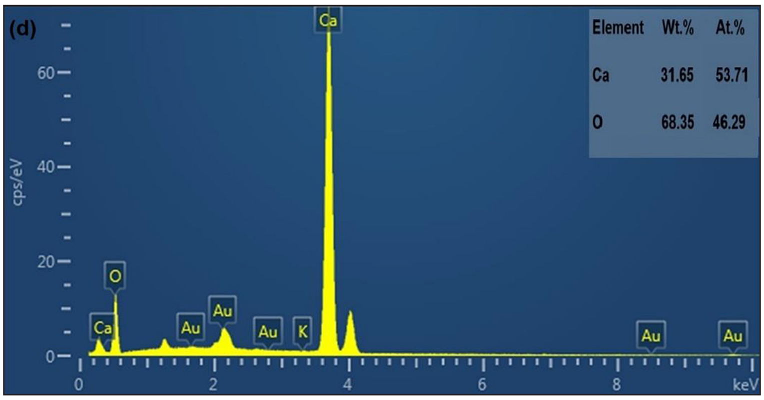

**Figure 5.** EXX mapping of the CES-derived NSBC

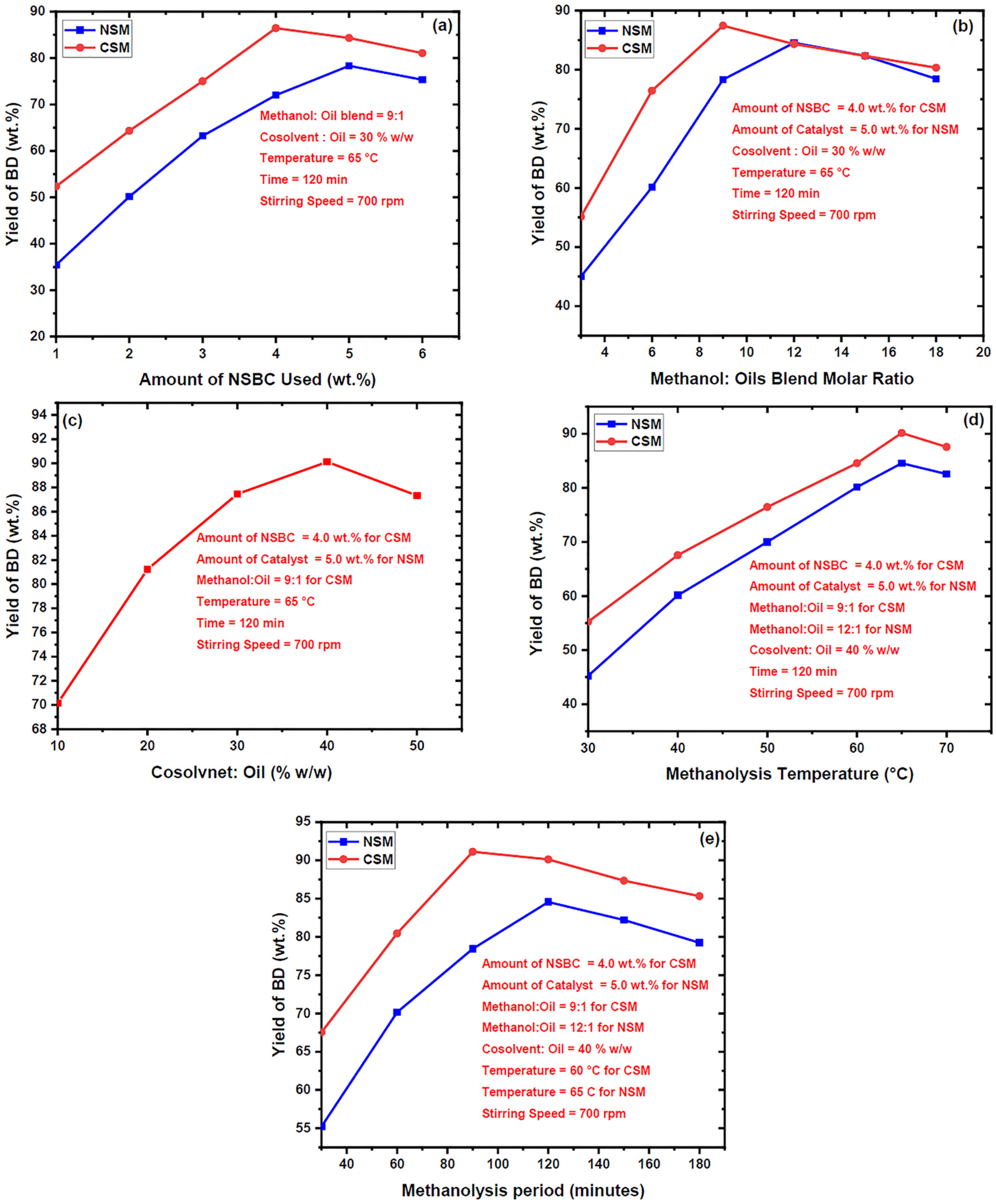

**Figure 6.** Effect of the CSM and NSM conditions on the yield of BD using NSBC

### The CSM and NSM of mixed oils NSBC

The CSM and NSM of mixed oils using the as-developed NSBC were accomplished, and the variables affecting the output of BD were optimized, as offered in Figure 6 (a-e).

The amount of the NSBC implemented in the CSM and NSM of the oils mix varied from 1.0 to 6.0 wt.%, while other conditions were kept unchanged, as presented in Figure 6a. The BD output increased with the increment of the NSBC amount via both routes. This outcome suggests that increasing the NSBC amount used in the methanolysis reaction will be associated with an increment in the active sites responsible for the reaction, leading to a better transformation of the parent mix of lipids into its corresponding ester (Fadhil et al., 2020). Based on the outcomes presented in Figure 6 (a), the CSM exhibited the highest yield of BD using a 4.0 wt.% of the NSBC, while the NSM produced the highest output of BD using 5.0 wt.% of the NSBC. Such a consequence could be ascribed to the co-solvent (n-hexane), whose presence within the methanolysis medium diminishes the oil's viscosity besides lowering the mass transfer limitations between the methanol and oils blend, leading to a better consequence (Saeed et al., 2021). These outcomes follow those established elsewhere (Fadhil et al., 2020). Nevertheless, the implementation of a higher dosage of the NSBC causes soaps formation, increases the transfer resistance, and retards the methanolysis reaction rate, leading to a lower output of BD (Chanakaewsomboon et al., 2020; Bai et al., 2022).

Evaluating the impact of the methanol: oil molar ratio on the BD yield was carried out by conducting multiple experiments using varied methanol: oil molar ratios (3:1 to 18:1) while keeping other settings fixed, as shown in Figure 6b. From this figure, the output of BD was enhanced by increasing the molar ratio of methanol to lipid using both approaches. For the CSM, the highest production of BD was obtained at a 9:1 molar ratio compared to 12:1 for the NSM. The cause behind these outcomes ascribes to the cosolvent, which increases the solubility of the blend in methanol, thus enhancing the reaction yield (Fadhil et al., 2020; Saeed et al., 2021). Nonetheless, beyond the typical molar ratio of methanol, a decline in the BD output was noticed as a consequence of the difficulty of separating BD and glycerin phases via gravity besides supporting the reverse reaction than BD creation (Fadhil et al., 2019; Ambat et al., 2020). Also, further amounts of alcohol will increase the production cost of BD (Fadhil et al., 2020). The obtained outcomes align with those established by other researchers (Ambat et al., 2020).

Although there are positive merits to involving the cosolvent within the reaction medium, its typical amount has to be optimized. As such, the weight percentage of cosolvent: oil involved in the methanolysis process was optimized by trying multiple percentages of hexane: oil (10–50% w/w), while other settings were preserved unchanged, as offered in Figure 6c. The latter showed an increment in the BD output when the amount of hexane increased from 10.0 wt.% to 40.0 wt.%, due to the use of the further amount of hexane will dilute the oils blend and thus diminishing its viscosity besides enhancing the interaction between the reactants, resulting in a decrement in the mass transfer resistances between the two phases (Fadhil et al., 2020; Saeed et al., 2021; Ambat et al., 2020; Singh et al., 2017). The typical ratio of hexane to methanol was 40.0 wt.%, as it produced the highest output of BD while trying higher ratios diminished the BD yield as an outcome of the dilution effect of the reactants (Fadhil et al., 2020; Ambat et al., 2020).

Inspecting the temperature's influence on the BD output produced via both CSM and NSM was accomplished at multiple temperatures (30 °C, 40 °C, 50 °C, 60 °C, 65 °C, and 70 °C). At the same time, other variables were preserved unchanged, as depicted in Figure 6d. The BD yield improved with the increment of the methanolysis temperature, due to rising temperature will be accompanied by a decrement in the system's viscosity, leading to a better collision among the reactants species, and thereby, the BD enhanced (Fadhil et al., 2020; Saeed et al., 2021). Nonetheless, the CSM exhibited the highest oils mix conversion into BD at 60 °C compared with 65 °C for the NSM. This outcome ascribes to the occurrence of cosolvent (hexane) in the reaction medium, which enhances interaction among the reactants by lowering the viscosity of the reactants (Saeed et al., 2021). However, temperatures above the typical ones caused a decline in the BD output owing to the saponification reaction of the oils blend in addition to the possibility of methanol and cosolvent evaporation, leading to a diminish in the BD yield (Fadhil et al., 2020; Ambat et al., 2020).

Various durations (30–180 min) were tried upon the CSM and NSM of the oils mix using the NSBC derived from CES, while other parameters were kept at their typical values. The outcomes presented in Figure 6e disclosed that the BD output enhanced using both routes while extending the methanolysis period. The CSM showed the highest conversion of mixed oils into BD at 90 min, compared with 120 min for the NSM. However, prolonging the process duration was accompanied by a decrement in the BD output due to the hydrolysis of the formed BD into soaps and free acids (Fadhil et al., 2020). The recombination of the glycerin with BD by extending the methanolysis duration is possible, leading to a decline in the BD output (Fadhil et al., 2020). A similar trend was announced by several authors during the CSM and NSM of various lipids in the literature (Fadhil et al., 2020).

## $^1$H NMR, FTIR, and TLC analysis of BD

Transformation of the said mixture of oils into BD using the so-developed NSBC was confirmed by various techniques, including $^1$H NMR and FTIR spectroscopy, besides the TLC technique. $^1$H NMR spectroscopy was implemented for the qualitative analysis of BD. Figure 7 offers the spectra of BD synthesized via CSM of mixed oils using the NSCB. The transformation of mixed oils into BD employing the NSBC was confirmed as an outcome of the occurrence of $\alpha$-$CH_2$ and $CH_3O$ protons at 2.25 and 3.62 ppm, respectively. Following Equation 2, the transformation of mixed WCO+WMO into BD under the optimal conditions of the CSM process amounted to 96.96%.

The most important functional groups in the pristine oils blend, and its derived BD sample produced under typical experimental conditions were analyzed using FTIR spectroscopy (Fig. 8). The FTIR spectra of the authentic blend and its derived BD indicated that the authentic feed and its derived BD were almost similar because they revealed the same distinguishing peaks, except the BD, which disclosed the occurrence of functional peaks of relating to the methyl ester. Generally, the blend showed absorption peaks between 2923–2853 cm$^{-1}$, attributing to the aliphatic C–H bond symmetric and asymmetric starching vibrations ($CH_2$ and $CH_3$). Also, the bending vibrations of the aliphatic C–H bond ($CH_2$ and $CH_3$) could be seen between 1436 –1237 cm$^{-1}$. The C–O stretching vibration of an ester group could be the absorption band located between 1160 –1033 cm$^{-1}$. The C=O stretching vibration of an ester was also detected in the FTIR spectra of the oils mix and was seen at 1743 cm$^{-1}$ (Bai et al., 2022; Fadhil et al., 2019; Banerjee et al., 2019; Elgharbawy et al., 2021). In the case of BD, the same functional groups were also detected with a variance in the intensity of some peaks to higher or lower wavenumbers, like the C=O group, whose intensity lessened to 1741 cm$^{-1}$. The characteristic peak, absent in the pristine feed spectrum but detected in the BD spectrum, was located at 1436 cm$^{-1}$. The occurrence of this band in the BD spectrum assured that the as-synthesized NSBC was effective in converting the parent mixed oils into its corresponding FAME (Fadhil et al., 2019; Banerjee et al., 2019; Elgharbawy et al., 2021). The

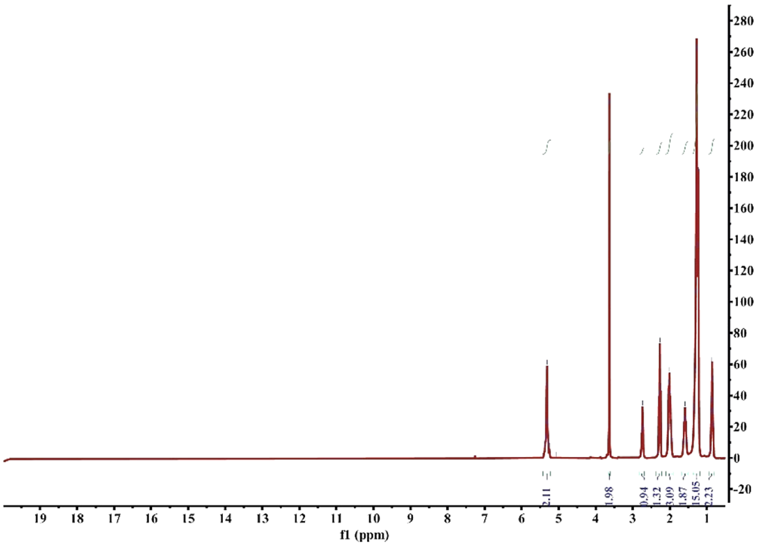

**Figure 7.** $^1$HNMR spectra of the resulting BD

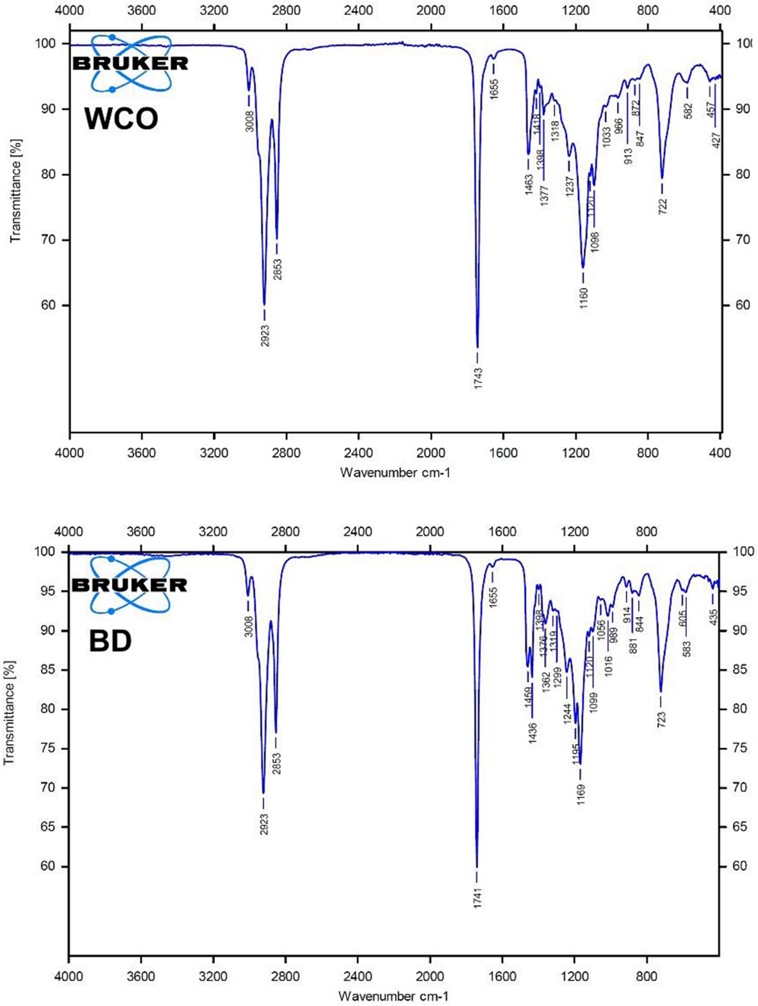

**Figure 8.** FTIR spectra of the oils blend and its derived BD

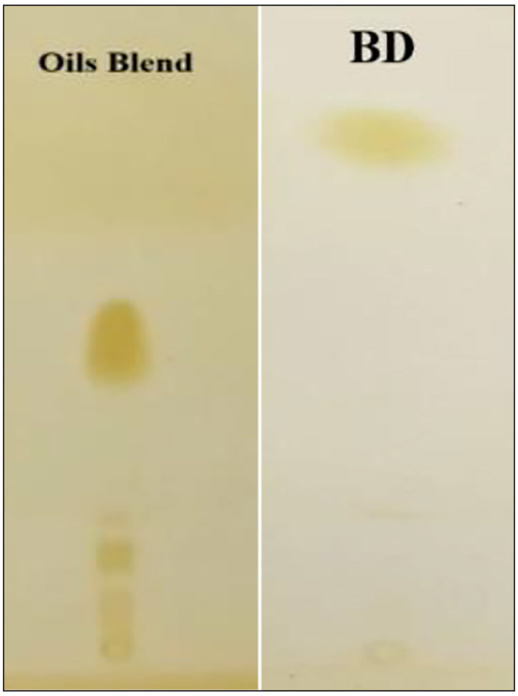

**Figure 9.** TLC images of the oils blend and its derived BD

absorption bands detected in the BD spectrum of the resulting BD were compatible with those established for BD samples produced from various lipids in the literature (Fadhil et al., 2019; Banerjee et al., 2019; Elgharbawy et al., 2021).

The TLC image of the parent mix of oils and its derived BD is depicted in Figure 9, which disclosed that three main spots could be detected in the feed at multiple flow rates ($R_f = 0.08$, 0.30 and 0.61 cm). These spots refer to the fractionation of pristine oils blended into mono-, di- or triglycerides, in addition to FFA. On the contrary, the BD exhibited one spot at various rates of flow ($R_f$ = 0.70 cm), which could be another piece of evidence of the transformation of the pristine lipid into BD (Fadhil et al., 2019).

## Comparison of typical activity of CaO nanocatalyst with other SBC samples

Table 1 lists a comparison of the conditions at which the highest output of BD was produced in this study with those of other SBC samples in the literature. From this table, the conditions required to produce the maximum yield of BD using the CaO nanocatalyst prepared in this study from CES were, in most cases, superior to those needed to exhibit the highest conversion of various lipids into BD. Here, these findings can be ascribed to several causes, including the type of lipid used in BD preparation and its acid value, the surface area of the CaO catalyst, the type of precursor used in the creation of CaO, and the type of the TE process (cosolvent-assisted or non-solvent). It can be seen through this study that among the main parameters that led to the production of higher output of BD is the presence of cosolvent, which played a positive role in achieving the highest conversion of mixed WCO+WMO into BD at mild conditions compared to other types of CaO catalyst. As we stated earlier, incorporating the cosolvent within the TE reaction medium has many merits, including increasing the solubility of the lipids in methanol. It also diminishes the oil's viscosity and lowers the mass transfer limitations between the methanol and oils blend. All these causes led to the production of high BD yield at mild conditions compared to those needed to yield the highest output of BD without cosolvent.

**Table 1.** The catalytic activity of NSBC compared with other SBC samples in the literature

| Oil | Catalyst | Conditions | Yield (wt.%) | Ref. |
|---|---|---|---|---|
| | | Cat. %; Methanol: oil; Temp.; Time; Cosolvent % | | |
| Palm oil | CaO from reiver snail shells | 10.0; 12:1; 65 °C; 90 min; 10.0 acetone | 98.0 | Roschat et al., 2016 |
| WCO | CaO from reiver snail shells | 3.0; 6:1; 65 °C; 180 min; 0.0 | 80.0 | Kedir et al., 2023 |
| WCO | $CaO/Al_2O_3$ | 4.0; 12:1; 65 °C; 300 min; 0.0 | 98.60 | Zabeti et al., 2009 |
| Soybean oil | CaO from Mussel shell | 4.0; 12:1; 60 °C; 480 min; 0.0 | 94.0 | Rezaei et al., 2013 |
| Soybean oil | CaO from reiver snail shells | 12.0; 24:1; 65 °C; 120 min; 20.0 acetone | 98.0 | Laskar et al., 2020 |
| Palm oil | CaO from Ostrich ES | 8.0; 9:1; 60 °C; 60 min; 0.0 | 92.70 | Wasserstein and Lazar, 2016 |
| Palm oil | CaO from Freshwater bivalve mussel shell | 4.0; 10:1; 60 °C; 300 min; 0.0 | 90.0 | Madhuvilakku et al., 2013 |
| Sunflower oil | CaO-ZnO | 2.0; 10:1; 60 °C; 240 min; 0.0 | 97.50 | Lau et al., 2016 |
| Palm kernel oil | CaO-ZnO | 10.0; 30:1; 60 °C; 60 min; 0.0 | 94.0 | Peng et al., 2018 |
| WCO+WMO | $K_2O$-CaO nanocatalyst | 5.0; 6:1; 60 °C; 60 min; 40.0 | 96.96 | This study |

**Table 2.** Fuel features of the BD samples compared with those of the parent feed

| Property | ASTM D-6751 | Oils Blend | BD from CSM | BD from NSM |
|---|---|---|---|---|
| D at 15.6 °C (mg/L) | 0.860–0.894 | 0.9188 | 0.8845 | 0.8921 |
| KV (40 °C, $mm^2$/sec) | 1.9–6.0 | 23.65 | 3.59 | 3.98 |
| FP (°C) | > 120 | 191.0 | 120.0 | 140.0 |
| PP (°C) | – | < -10.0 | < -10.0 | < -10.0 |
| AV (mg KOH/g) | ≤ 0.5 | 1.21 | 0.20 | 0.23 |

### Fuel properties of BD samples

For BD to be employed as an alternative to diesel fuel, its fuel properties, like those tabulated in Table 2, must conform to those established by the ASTM D6751 requirements. Accordingly, these properties were measured and compared with the parent oils blend.

It is apparent from Table 2 that the CSM and NSO of the oils blend using the as-synthesized NSBC were able to positively alter the authentic features of the parent mix of oils. The D values for BD samples were below those measured for the authentic feed. Similarly, the KV values were much below those observed for the native oils mix. The CSM lessened the D of the native oils mix by around 3.73% compared with 2.90% for NSM, while the reduction in the KV after the CSM of mixed WCO+WMO amounted to 84.8% compared with 83.17% for the NSM. Such outcomes suggest that the atomization of the produced fuels will be easier. On the other hand, the FP of the parent mix of oils dropped by around 37.17% after the CSM compared with 26.70% for the NSM. The higher FP values for the BD sample suggest that they are safer than petrodiesel. Finally, the decrease in the AV of the pristine WCO+WMO through the CSM and NSM were respectively 83.47% and 80.90%. According to the obtained findings, the NSBC developed was very effective in enhancing the fuel features of the parent mixture of oils through the CSM and NSM processes so that these features conformed to those recognized by the ASTM standards, and thereby, the resulting BD samples could be employed as a successful alternative to petrodiesel. Also, according to the outcomes tabulated in Table 2, the CSM caused an energetic drop in the fuel properties of the authentic oils blend compared to the NSM. These findings belong to the occurrence of the co-solvent within the reaction medium, which positively affects the TE reaction, as stated earlier, which in turn led to a higher transformation of the oils mix into BD.

### Reusability of the spent NSBC

For economic and ecological concerns, the reusability of any SBC is a critical factor besides affecting the production cost of BD (Ashine et al., 2023). Accordingly, the exhausted NSBC developed from the CES was regenerated and reused in the CSM of the oils blend for 5 cycles, and the experiments were carried out under the conditions presented in Figure 10. Findings presented in this figure indicated a diminish in the BD output with the increment of the reuse cycles. This reduction in the BD output might be ascribed to the posing of the catalytic active sites of the catalyst by the oil and glycerin molecules, resulting in a limited contact area between the reactants and active sites of the catalyst, and thus declined the BD yield (Yusuff et al., 2021). Also, the repeated washing of the spent catalyst to get rid of the oil species from the catalyst pores, besides calcination, caused a decrement in the number of active sites available for the reaction, thereby lessening the output of BD. Furthermore, the repeated washing of the spent catalyst with methanol in addition to the calcination will leach calcium-active species from the catalyst surface, thus decreasing the BD yield (Pandit and Fulekar, 2019). Results indicate that CaO from consumed CES could be utilized as an ecofriendly catalyst for the production of BD.

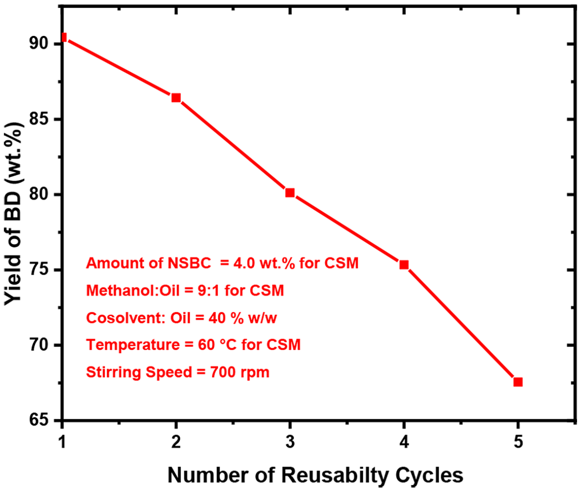

**Figure 10.** Reusability experiments of the regenerated NSBC

## CONCLUSIONS

This work accomplished the cosolvent methanolysis (CSM) and non-solvent methanolysis (NSM) reaction of mixed WCO+WMO using the NSBC developed from CES after being calcinied at 850 °C for 2 h at a 10 °C/min rate of heating. Diverse techniques identified the NSBC, and the outcomes disclosed that it had a BET surface area of 11.47 $m^2/g$ and an average pore diameter of 8.12 nm, suggesting its mesoporous structure, which is helpful for the methanolysis reaction of lipids. The CSM of the oils blend produced the highest output of BD (91.12%) using 4.0 wt.% of the NSBC, 9:1 methanol: oil molar ratio, 40 wt.% of cosolvent, 60 °C, and 1.5 h, while the NSM of the oils blend produced the highest yield of BD (84.55%) at 65 °C for 2 h using 5.0 wt.% of the NSBC and 12:1 methanol: oil molar ratio. Analysis of BD employing FTIR spectroscopy and TLC technique confirmed the oil blend transformation into BD. Quantifying mixed oils transformation into BD amounted to 96.96% based on the $^1$HNMR spectroscopy measurements. Besides, the fuel properties of the resulting BD conformed to those established for the ASTM D-6751 BD. In conclusion, the NSBC catalyst could be utilized as an effective catalyst for the methanolysis reaction of lipids. Also, the presence of cosolvent within the reaction medium effectively reduced the experimental conditions required to achieve the highest transformation of the oils blend into BD compared to the NSM process.

## Acknowledgements

Mosul University, College of Science, Chemistry Department are highly appreciated by the authors for supporting this work.

## REFERENCES

1. Ahmad, S., Chaudhary, S., Pathak, V. V., Kothari, R., & Tyagi, V. V. (2020). Optimization of direct transesterification of Chlorella pyrenoidosa catalyzed by waste egg shell based heterogenous nano–CaO catalyst. *Renewable Energy*, *160*, 86–97.
2. Al-Tikrity, E. T, Fadhil, A. B., Dheyab M. M. (2015). Two-step Base Catalyzed Transesterification of Chicken Fat: Optimization of Parameters. *Energy Sources, Part A: Recovery, Utilization, and Environmental Effects, 37*(17), 1861–1866.
3. Ambat, I., Srivastava, V., Iftekhar, S., Haapaniemi, E., & Sillanpää, M. (2020). Effect of different cosolvents on biodiesel production from various low-cost feedstocks using Sr–Al double oxides. *Renewable Energy*, *146*, 2158–2169.
4. Annane, K., Lemlikchi, W., & Tingry, S. (2023). Efficiency of eggshell as a low-cost adsorbent for removal of cadmium: Kinetic and isotherm studies. *Biomass Conversion and Biorefinery*, *13*(7), 6163–6174.
5. Ashine, F., Kiflie, Z., Prabhu, S. V., Tizazu, B. Z., Varadharajan, V., Rajasimman, M.,... & Jayakumar, M. (2023). Biodiesel production from Argemone mexicana oil using chicken eggshell derived CaO catalyst. *Fuel*, *332*, 126166.
6. Bai, H., Tian, J., Talifu, D., Okitsu, K., & Abulizi, A. (2022). Process optimization of esterification for deacidification in waste cooking oil: RSM approach and for biodiesel production assisted with ultrasonic and solvent. *Fuel*, *318*, 123697.
7. Banerjee, S., Sahani, S., & Sharma, Y. C. (2019). Process dynamic investigations and emission analyses of biodiesel produced using Sr–Ce mixed metal oxide heterogeneous catalyst. *Journal of environmental management*, *248*, 109218.
8. Buasri, A., Rattanapan, T., Boonrin, C., Wechayan, C., & Loryuenyong, V. (2015). Oyster and Pyramidella Shells as Heterogeneous Catalysts for the Microwave-Assisted Biodiesel Production from Jatropha curcas Oil. *Journal of Chemistry*, *2015*(1), 578625.
9. Chanakaewsomboon, I., Tongurai, C., Photaworn, S., Kungsanant, S., & Nikhom, R. (2020). Investigation of saponification mechanisms in biodiesel production: Microscopic visualization of the effects of FFA, water and the amount of alkaline catalyst. *Journal of Environmental Chemical Engineering*, *8*(2), 103538.
10. Chumuang, N., & Punsuvon, V. (2017). Response surface methodology for biodiesel production using calcium methoxide catalyst assisted with tetrahydrofuran as cosolvent. *Journal of Chemistry*, *2017*(1), 4190818.
11. da Conceição, L. R. V., da Costa, C. E. F., Filho, G. N. D. & Filho, E. R. P. J. R. (2015). Ethanolysis optimisation of jupati (Raphia taedigera Mart.) oil to biodiesel using response surface methodology. *Journal of the Brazilian Chemical Society*, *26*, 1321–1330.
12. Danane, F., Bessah, R., Alloune, R., Tebouche, L., Madjene, F., Kheirani, A. Y., & Bouabibsa, R. (2022). Experimental optimization of Waste Cooking Oil ethanolysis for biodiesel production using Response Surface Methodology (RSM). *Science and Technology for Energy Transition*, *77*, 14.
13. Deharbe M. Milagros, M., Gómez, L. E., Boix, A. V., & Serra, R. M. (2023). Synthesis and characterization of eggshell-based catalysts for the treatment of gaseous pollutants. *Applied Catalysis A: General*, *668*, 119471.
14. Elgharbawy, A. S., Sadik, W. A., Sadek, O. M., & Kasaby, M. A. (2021). Glycerolysis treatment to enhance biodiesel production from low-quality feedstocks. *Fuel*, *284*, 118970.
15. Fadhil, A.B., Al-Tikrity, E.T.B., Ibraheem, K.K. (2019). Transesterification of bitter almond oil as a new non-edible feedstock with mixed alcohols system: Parameter optimization and analysis of biodiesel. *Waste and Biomass Valorization*, *10*, 1597–1608.
16. Fadhil, A. B., Nayyef, A. W., & Al-Layla, N. M. (2020). Biodiesel production from nonedible feedstock, radish seed oil by cosolvent method at room temperature: evaluation and analysis

of biodiesel. *Energy Sources, Part A: Recovery, Utilization, and Environmental Effects*, *42*(15), 1891–1901.

17. Gupta A. R., Rathod V. K. (2018). Waste cooking oil and waste chicken eggshells derived solid base catalyst for the biodiesel production: optimization and kinetics. Waste Manage 79, 169–78.
18. Huang, J., Zou, Y., Yaseen, M., Qu, H., He, R., & Tong, Z. (2021). Fabrication of hollow cage-like CaO catalyst for the enhanced biodiesel production via transesterification of soybean oil and methanol. *Fuel*, *290*, 119799.
19. Jamil, F., Al-Riyami, M., Al-Haj, L., Al-Muhtaseb, A. A. H., Myint, M. T., Baawain, M., & Al-Abri, M. (2021). Waste Balanites aegyptiaca seed oil as a potential source for biodiesel production in the presence of a novel mixed metallic oxide catalyst. *International Journal of Energy Research*, *45*(12), 17189–17202.
20. Kedir, W. M., Wondimu, K. T., & Weldegrum, G. S. (2023). Optimization and characterization of biodiesel from waste cooking oil using modified CaO catalyst derived from snail shell. *Heliyon*, *9*(5).
21. Khan, S. G., Hassan, M., Anwar, M., Khan, U. M., & Zhao, C. (2022). Mussel shell based CaO nano-catalyst doped with praseodymium to enhance biodiesel production from castor oil. *Fuel*, *330*, 125480.
22. Laskar, I. B., Deshmukhya, T., Bhanja, P., Paul, B., Gupta, R., & Chatterjee, S. (2020). Transesterification of soybean oil at room temperature using biowaste as catalyst; an experimental investigation on the effect of co-solvent on biodiesel yield. *Renewable Energy*, *162*, 98–111.
23. Lau, P. C., Kwong, T. L., & Yung, K. F. (2016). Effective heterogeneous transition metal glycerolates catalysts for one-step biodiesel production from low grade non-refined Jatropha oil and crude aqueous bioethanol. *Scientific reports*, *6*(1), 23822.
24. Madhuvilakku, R., Mariappan, R., Jeyapal, S., Sundar, S., & Piraman, S. (2013). Transesterification of palm oil catalyzed by fresh water bivalve mollusk (Margaritifera falcata) shell as heterogeneous catalyst. *Industrial & Engineering Chemistry Research*, *52*(49), 17407–17413.
25. Maneechakr, P., & Karnjanakom, S. (2021). Systematic production of biodiesel fuel from palm oil over porous K2O@ CaO catalyst derived from waste chicken eggshell via RSM/kinetic/thermodynamic studies. *Journal of Environmental Chemical Engineering, 9*(6), 106542.
26. Mannu, A., Ferro, M., Pietro, M. E. D., & Mele, A. (2019). Innovative applications of waste cooking oil as raw material. *Science progress*, *102*(2), 153–160.
27. Mares, E. K. L., Gonçalves, M. A., da Luz, P. T. S., da Rocha Filho, G. N., Zamian, J. R., & da Conceição, L. R. V. (2021). Acai seed ash as a novel basic heterogeneous catalyst for biodiesel synthesis: Optimization of the biodiesel production process. *Fuel*, *299*, 120887.
28. Mohadesi, M., Aghel, B., Maleki, M., & Ansari, A. (2020). Study of the transesterification of waste cooking oil for the production of biodiesel in a microreactor pilot: The effect of acetone as the co-solvent. *Fuel*, *273*, 117736.
29. Navas, M. B., Ruggera, J. F., Lick, I. D., & Casella, M. L. (2020). A sustainable process for biodiesel production using Zn/Mg oxidic species as active, selective and reusable heterogeneous catalysts. *Bioresources and Bioprocessing*, *7*, 1–13.
30. Nguyen, H. C., Liang, S. H., Li, S. Y., Su, C. H., Chien, C. C., Chen, Y. J., & Huong, D. T. M. (2018). Direct transesterification of black soldier fly larvae (Hermetia illucens) for biodiesel production. *Journal of the Taiwan Institute of Chemical Engineers*, *85*, 165–169.
31. Pandit, P. R., & Fulekar, M. H. (2017). Egg shell waste as heterogeneous nanocatalyst for biodiesel production: optimized by response surface methodology. *Journal of environmental management*, *198*, 319–329.
32. Pandit, P. R., & Fulekar, M. H. (2019). Biodiesel production from microalgal biomass using CaO catalyst synthesized from natural waste material. *Renewable Energy*, *136*, 837–845.
33. Paruthi, S., Khan, A. H., Kumar, A., Kumar, F., Hasan, M. A., Magbool, H. M., & Manzar, M. S. (2023). Sustainable cement replacement using waste eggshells: A review on mechanical properties of eggshell concrete and strength prediction using artificial neural network. *Case Studies in Construction Materials*, *18*, e02160.
34. Peng, Y. P., Amesho, K. T., Chen, C. E., Jhang, S. R., Chou, F. C., & Lin, Y. C. (2018). Optimization of biodiesel production from waste cooking oil using waste eggshell as a base catalyst under a microwave heating system. *Catalysts*, *8*(2), 81.
35. Rezaei, R., Mohadesi, M., & Moradi, G. R. (2013). Optimization of biodiesel production using waste mussel shell catalyst. *Fuel*, *109*, 534–541.
36. Roschat, W., Siritanon, T., Kaewpuang, T., Yoosuk, B., & Promarak, V. (2016). Economical and green biodiesel production process using river snail shells-derived heterogeneous catalyst and co-solvent method. *Bioresource technology*, *209*, 343–350.
37. Sahani, S., Banerjee, S., & Sharma, Y. C. (2018). Study of'co-solvent effect'on production of biodiesel from Schleichera Oleosa oil using a mixed metal oxide as a potential catalyst. *Journal of the Taiwan Institute of Chemical Engineers*, *86*, 42–56.
38. Sajadi, S. M., Kolo, K., Abdullah, S. M., Hamad, S. M., Khalid, H. S., & Yassein, A. T. (2018). Green synthesis of highly recyclable CuO/eggshell nanocomposite to efficient removal of aromatic containing compounds and reduction of 4-nitrophenol at room

temperature. *Surfaces and Interfaces, 13*, 205–215.

39. Shan, R., Chen, G., Yan, B., Shi, J., & Liu, C. (2015). Porous CaO-based catalyst derived from PSS-induced mineralization for biodiesel production enhancement. *Energy Conversion and Management*, *106*, 405–413.
40. Singh, V., Yadav, M., & Sharma, Y. C. (2017). Effect of co-solvent on biodiesel production using calcium aluminium oxide as a reusable catalyst and waste vegetable oil. *Fuel*, *203*, 360–369.
41. Tanpure, S., Ghanwat, V., Shinde, B., Tanpure, K., & Lawande, S. (2022). The eggshell waste transformed green and efficient synthesis of K-Ca (OH) 2 catalyst for room temperature synthesis of chalcones. *Polycyclic Aromatic Compounds*, *42*(4), 1322–1340.
42. Usman, M., Salama, E. S., Arif, M., Jeon, B. H., & Li, X. (2020). Determination of the inhibitory concentration level of fat, oil, and grease (FOG) towards bacterial and archaeal communities in anaerobic digestion. *Renewable and Sustainable Energy Reviews*, *131*, 110032.
43. Wasserstein, R. L., & Lazar, N. A. (2016). The ASA statement on p-values: context, process, and purpose. *The American Statistician, 70*(2), 129–133.
44. Yan, S., Kim, M., Salley, S. O., & Ng, K. S. (2009). Oil transesterification over calcium oxides modified with lanthanum. *Applied Catalysis A: General*, *360*(2), 163–170.
45. Yusuff, A. S., Gbadamosi, A. O., & Popoola, L. T. (2021). Biodiesel production from transesterified waste cooking oil by zinc-modified anthill catalyst: Parametric optimization and biodiesel properties improvement. *Journal of Environmental Chemical Engineering*, *9*(2), 104955.
46. Zabeti, M., Daud, W. M. A. W., & Aroua, M. K. (2009). Optimization of the activity of CaO/Al2O3 catalyst for biodiesel production using response surface methodology. *Applied Catalysis A: General*, *366*(1), 154–159.
47. Zhang, S., Han, A., Zhai, Y., Zhang, J., Cheong, W. C., Wang, D., & Li, Y. (2017). ZIF-derived porous carbon supported Pd nanoparticles within mesoporous silica shells: sintering-and leaching-resistant core–shell nanocatalysts. *Chemical Communications*, *53*(68), 9490–9493.